A Comparative Study of the Effect of Strain on the Electronic and Optical Properties of Filled and Unfilled Ba$_8$Si$_{46}$ Type I-clathrate

N.A. Mahammedi[a,b,], R. Belkada[c] and M. Ferhat[b,d]

[a]Laboratoire de Physique des Matériaux LPM, Amar Télidji University of Laghouat,
BP 37G, Laghouat 03000, Algeria

[b]Semiconductors and Functional Materials Laboratory SFML, Amar Télidji University, Laghouat,

[c]CRTSE, Research Center in Semiconductor Technology for the Energetic, Algiers, Algeria

[d]Department of Physics, University of the West Indies, Kingston 07, Jamaica

A first principles calculations study is carried out to theoretically investigate the effect of compressive and tensile strains on the structural, electronic and optical properties of type-I guest-free Si$_{46}$ and barium-filled Ba$_8$Si$_{46}$ clathrates. The electronic band structure of the unfilled Si$_{46}$ clathrate revealed a semiconducting behaviour with a quasi-direct band gap of 1.36 eV. Under hydrostatic pressure, the bandgap magnitude of the guest-free Si$_{46}$ behaves monotonously. For the Ba doped Si$_{46}$ clathrate (Ba$_8$Si$_{46}$) structure, the strain has no significant effect on the electronic band structure, while its impact on the optical properties is appreciable. The optical properties, such as the dielectric function and the absorption were computed for different strain variations, which are clearly enhanced for both the unfilled Si$_{46}$ and Ba-filled Ba$_8$Si$_{46}$ clathrates when the pressure is 1 GPa in the direction of a compressive state.

1. Introduction

Group-IV inorganic clathrates are cage-like materials where a number of host atoms form a network arranged in cage shape to possibly enclose a guest atom. Indeed, this class of material is very promising given the large possibilities to tune the intrinsic properties by substituting both host and guest atoms in order to design new materials having desired functions for specific applications. Depending on the atomic arrangements eight types of clathrates are well established [1]. The type-I structure is the most investigated among the different known types, on the other hand, it has an excellent thermoelectric [1], semiconducting, and superconducting properties [2]. Guest free type-I Si$_{46}$ silicon clathrate is a hypothetical structure, which has been theoretically studied and expected to exhibit interesting thermoelectric and electronic properties as a promising semiconductor material with a band-gap greater than that of silicon in the diamond structure [3]. However, the actual synthesis of type-I Si$_{46}$ clathrate remains a challenging task and yet not resolved. In contrast with type-I Si$_{46}$ silicon clathrate, the filled Ba$_8$Si$_{46}$ [4] and partially vacant Ba$_x$Si$_{46}$ [5] have been synthesized by different methods, mostly by using techniques based on high pressure and high temperature. The synthesized Ba$_8$Si$_{46}$ material revealed several technological properties, especially it is known as the first clathrate to demonstrate low temperature superconductivity, in addition, by partial substitution of barium with aluminium, Ba$_8$Si$_{46}$ have showed a good semiconducting behaviour [5]. One drawback of
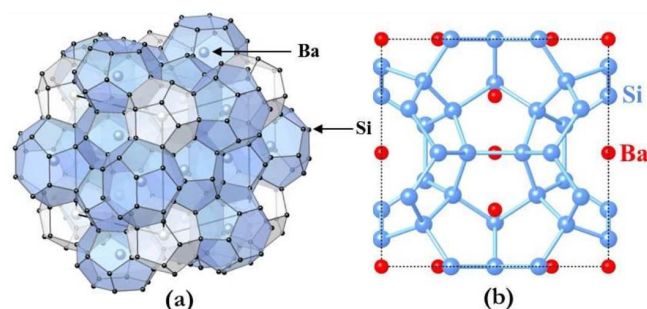

Fig. 1. Atomic configuration of Ba$_8$Si$_{46}$ structure formed by polyhedrons network in (a) and the unit given in (b). Ba and Si atoms are shown respectively in red and in blue color.

this material is related to its low mechanical properties under hydrostatic pressure.

In this work we have systematically investigated the effect of hydrostatic pressure on the electronic and optical properties of Ba$_8$Si$_{46}$ and Si$_{46}$ clathrates in type-I configurations by using first principles calculations in the frame of density functional theory (DFT). The development of the computational techniques for applying DFT to real materials has made it possible to predict quantitatively the atomic and electronic structure and properties of different materials [6–10]. In particular, the pseudopotential method based on the local DFT [7–11] has been very successfully used for studying various properties of the crystals [8], surfaces, and interfaces of metals, ceramics, and semiconductors [12]. The first part deals with

a concise description of the theoretical background; in the second part the structural and electronic aspects of both compounds were examined.

2. Calculation methods

Inorganic clathrates are mainly composed from face-sharing polyhedral networks of group IV atoms (C, Si, Ge, and Sn), entrapping guest atoms like alkaline-earth, rare-earth or alkali-metals, among others. The type-I configuration with formula is X_8A_{46} (X = guest, A = group IV) belongs to the simple cubic in $Pm3n$ space group, build-up from association of dodecahedron and tetrakaedicahedron polyhedrons networks as directed in Fig. 1, where host atoms occupy the 2a, 6c, 16i, and 24k symmetric positions, whereas the guest atom species (X) are located in 6d positions according to the Wyckoff designation.

In the present work a first-principles calculation is carried out using Cambridge Serial Total Energy Package (CASTEP) [13] code, based on the DFT [14, 15]. To describe the electric wave function, a plane-wave ultra-soft pseudopotential method is adopted. For the energy minimization the generalized gradient approximation (GGA) is used within the Perdew–Burke–Erzenhorf (PBE) [16] approach. In the present calculation, for accuracy we have set a plane-wave cut-off energy value to 480 eV, and the first irreducible Brillouin zone in the reciprocal space was sampled using $6 \times 6 \times 6$ grid mesh following the Monkhorst–Pack scheme resulting to a total number of 108 k-points. In order to obtain optimal geometrical parameters and internal coordinates, a rigorous atomic relaxation of the system is performed using the Broyden–Fletcher–Goldfarb–Shanno (BFGS) [17–20] optimization algorithm until obtaining the Hellmann–Feynman atomic forces with a value lower than 10^{-3} eV/Å. Optical properties were computed for each step of the hydrostatic pressure using $14 \times 14 \times 14$ mesh points sampling in the first Brillouin zone for better approximation of the dielectric function.

For the calculated mechanical properties to simulate hydrostatic pressure, an isotropic stress tensor is exerted on the system, the strain response is defined through the Moore law of general elasticity given as follows: $(\sigma_{ij}) = (C_{ij})(\varepsilon_{ij})$, $i, j = 1, 2, 3$, where σ_{ij} are the elements of the tensor matrix, C_{ij} are the elastic constants, and the ε_{ij} represent the elements of the strain tensor. The cubic nature of the type-I lattice leads to define only three elastic constants, i.e. C_{11}, C_{12} and C_{44} which are equal to: $C_{11} = 135$ GPa, $C_{12} = 58$ GPa, and $C_{44} = 40$ GPa as reported in the literature for both Si_{46} and Ba_8Si_{46} clathrates [4]. In the present calculation we have simulated hydrostatic pressure values between –3% to +3% by a variation step of 1%.

3. Results and discussion

We have calculated the structural properties of both Ba_8Si_{46} and Si_{46} structures considering both applied hydrostatic pressure and without pressure. Knowing the fact that GGA–PBE calculations underestimate lattice constants and internal coordinates, as shown in Table I, our calculated results exhibit a good agreement with available experimental and other theoretical results. The calculated lattice constants are of $a = 10.0$ Å and $a = 10.22$ Å for the unstrained Ba_8Si_{46} and Si_{46} structures, respectively. Depending on whether compressive or tensile strain is applied, we have found that the lattice parameters vary monotonously with the magnitude of the applied hydrostatic pressure. In our case, the simulated hydrostatic pressure for Be_8Si_{46} do not exceed 15 GPa as reported in [9], which can undergo phase transformation beyond this limit. As for Si_{46} clathrate, the value of 19 GPa is defined as an upper limit referenced to the theoretically predicted in [10]. The calculated structural, electronic, and optical properties for both Ba_8Si_{46} and Si_{46} structure are considered taking into account these limited values of hydrostatic pressures.

TABLE I

Calculated lattice parameter for type–I Ba_8Si_{46} and Si_{46} clathrates structures (GGA–PBE), space group No. 223 (Pm-$3n$). [a] — this work, (GGA–PBE)

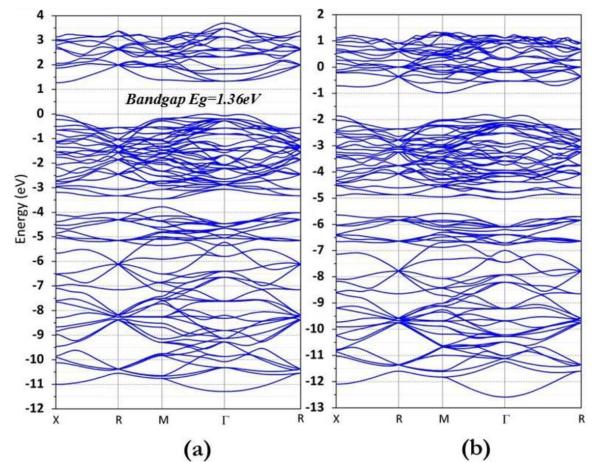| Ba_8Si_{46}–I	Si_{46}–I
10.31[a], 10.328 [11], 10.3177 [12]	10.22[a], 10.20 [10], 10.055 [13]

Fig. 2. GGA-PBE calculated energy band structure for the type-I (unfilled) Si_{46} (a) and for the Ba (filled) Ba_8Si_{46} (b).

Figure 2 shows the calculated band structure along X–R–M–G–M high symmetry path of the first irreducible Brillouin zone for the type-I Si_{46} and Ba_8Si_{46} structures under zero hydrostatic pressure. Figure 2a reveals an indirect band gap of 1.36 eV in which the valence band maximum is located between M and G high symmetry points, while the conduction band minimum is located at the X point. The Si_{46} clathrate exhibits a semiconducting character as supported by previous theoretical studies. The transition from semiconducting behaviour to metallic character is observed due to the inclusion of Ba atom as shown in the obtained band structure of Ba_8Si_{46} depicted in Fig. 2b, which results in the mixture, near to the Fermi level, of the 3d states of Ba and 2p from Si in the Ba–Si bonding. For the case of applied
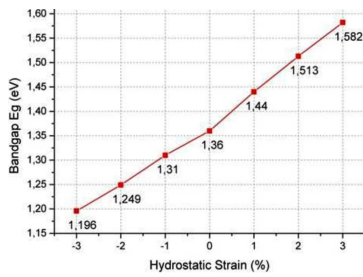
Fig. 3. Variation of the band-gap as a function of hydrostatic pressure for type-I Si_{46} obtained by GGA-PBE approximation.

tensile or compressive hydrostatic pressures, the energy band gap in Si_{46} remains quasidirect, and exhibits minor changes in the energy position of the VBM and CBM, however, the band gap magnitude varies quasi-linearly with the applied strain.

The variation of band gap magnitude as a function of applied pressure is shown in Fig. 3. Under the applied hydrostatic pressure, the band gap magnitude changes monotonously with varying from –3% to +3% described in Fig. 3. For the case of filled Ba_8Si_{46}, the applied hydrostatic pressure slightly affects the interatomic distances and cell volumes keeping a monotonous variation with the incremented pressure magnitude. Nevertheless, the effect of the pressure on Ba_8Si_{46} modify its optical properties, in particular the complex dielectric function. Figure 4 illustrates the dielectric functions of Ba_8Si_{46} as function of the photon energy for Ba_8Si_{46} showing respectively the real (Fig. 4a) and imaginary (Fig. 4b) parts of dielectric function for different values of hydrostatic pressure (0, 1, 3, 5, and 7 GPa). It is observed from Fig. 4b that the value ε_2 tends to zero more rapidly for the higher pressure in the examined ranges. Figure 4b indicates that the material is susceptible to become transparent at low energy value. It is clear that from Fig. 4 the simulated 1 GPa gives better optical properties as compared to other higher values.
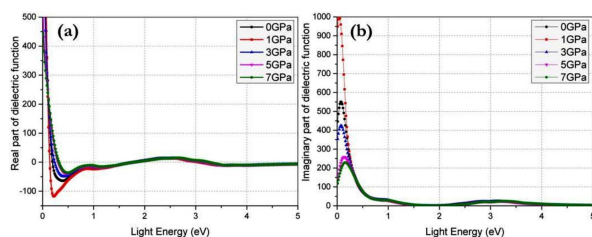

Fig. 4. Calculated GGA-PBE real (a) and imaginary (b) part of the dielectric function as functions of hydrostatic pressure for the type-I filled Ba_8Si_{46}.

4. Conclusion

In the present study, we have systematically investigated by performing DFT calculations, the structural, electronic and optical properties of the unfilled Si_{46} and filled Ba_8Si_{46} type-I clathrates under various pressures. The calculated lattice parameters for both structures Si_{46}

and Ba_8Si_{46} are in good agreement with the experimental and former theoretical results. The electronic band structure shows a semiconducting character for Si_{46} structure with a quasi-direct band gap, which turns to a metallic character due to the presence of the Ba atoms. We have found that under the simulated pressure the band gap in Si_{46} remains quasi-direct and its magnitude change noticeably with the pressure variation, while the pressure is less affecting the electronic properties of Ba_8Si_{46} but appreciable for its optical properties.

References

[1] J-A. Dolyniuk, B. Owens-Baird, Jian Wang, J.V. Zaikina, K. Kovnir, *Mat. Sci. Eng. R: Rep.* **108**, 46 (2016).

[2] Wei-Qiang Cao, Yong-Gao Yan, Xin-Feng Tang, Shu-Kang Deng, *J. Phys. D Appl. Phys.* **41**, 215105 (2008).

[3] Y. Imai, M. Imai, *J. Alloys Comp.* **509**, 3924 (2011).

[4] H. Fukuoka, J. Kiyoto, S. Yamanaka, *J. Solid State Chem.* **175**, 237 (2003).

[5] A. Kitano, K. Moriguchi, M. Yonemura, S. Munetoh, A. Shintani, H. Fukuoka, S. Yamanaka, E. Nishibori, M. Takata, M. Sakata, *Phys. Rev. B* **64**, 045206 (2001).

[6] Ying Liang, B. Böhme, L. Vasylechko, M. Baitinger, Y. Grin, *J. Phys. Chem. Solids* **74**, 225 (2013).

[7] N. Kaya Kinaytürk, H. Oturak, *Acta Phys. Pol. A* **130**, 276 (2016).

[8] H. Oturak, N. Kaya Kinaytürk, G. Şahın, *Acta Phys. Pol. A* **128**, B-417 (2016).

[9] R. Belkada, T. Shibayanagi, M. Naka, *J. Am. Ceram. Soc.* **83**, 2449 (2000).

[10] R. Belkada, M. Kokyama, T. Shibayanagi, M. Naka, *Phys. Rev. B* **65**, 092104 (2002).

[11] H.K. Dipojono, A.G. Saputro, R. Belkada, H. Nakanishi, H. Kasai, M. David, E. Sy Dy, *J. Phys. Soc. Jpn.* **78**, 094710 (2009).

[12] W.T. Cahyanto, F. Oemry, A.A.B. Padama, M. Sakaue, R. Belkada, S.M. Aspera, M. Chikaishi, S. Kunikata, H. Nakanishi, H. Kasai, H. Maekawa, K. Osumi, Y. Tashiro, *Jpn. J. Appl. Phys.* **50**, 105602 (2011).

[13] S.J. Clark, M.D. Segall, C.J. Pickard, P.J. Hasnip, M.I.J. Probert, K. Refson, M.C. Payne, *Z. Kristallogr.* **220**, 567 (2005).

[14] P. Hohenberg, W. Kohn, *Phys. Rev.* **136**, B864 (1964).

[15] W. Kohn, L.J. Sham, *Phys. Rev.* **140**, A1133 (1965).

[16] L. Yang, Y.M. Ma, T. Iitaka, J.S. Tse, K. Stahl, Y. Ohishi, Y. Wang, R.W. Zhang, J.F. Liu, H.-K. Mao, J.Z. Jiang, *Phys. Rev. B* **74**, 455 (2006).

[17] M. Menon, E. Richter, K. Subbaswamy, *Phys. Rev. B* **56**, 12290 (1997).

[18] A. San-Miguel, P. Toulemonde, *High Press. Res.* **25**, 159 (2005).

[19] P. Toulemonde, A. San Miguel, A. Merlen, R. Viennois, S. Le Floch, Ch. Adessi, X. Blase, J.L. Tholence, *J. Phys. Chem. Solids* **67**, 1117 (2006).

[20] D. Kahn, J. Ping Lu, *Phys. Rev. B* **56**, 13898 (1997).